High-velocity frictional properties of clay-rich fault gouge in a megasplay fault zone, Nankai subduction zone

Kohtaro Ujiie[1] and Akito Tsutsumi[2]

Received 28 October 2010; accepted 8 November 2010; published 29 December 2010.

[1] We conducted high-velocity friction experiments on clay-rich fault gouge taken from the megasplay fault zone in the Nankai subduction zone under dry and wet conditions. In the dry tests, dehydration of clay minerals occurred by frictional heating, and slip weakening is related to thermal pressurization associated with water vaporization, resulting in a random distribution of clay-clast aggregates in the gouge matrix. In the wet tests, slip weakening is caused by pore-fluid pressurization via shear-enhanced compaction and frictional heating, and there is a very weak dependence of the steady-state shear stress on the normal stress. The resulting microstructure reflects the grain size segregation in a granular-fluid shear flow at high shear rates. These results suggest that earthquake rupture propagates easily through clay-rich fault gouge by high-velocity weakening, potentially leaving the microstructures resulting from the frictional heating or the flow sorting at high slip rates.
Citation: Ujiie, K., and A. Tsutsumi (2010), High-velocity frictional properties of clay-rich fault gouge in a megasplay fault zone, Nankai subduction zone, *Geophys. Res. Lett.*, *37*, L24310, doi:10.1029/2010GL046002.

1. Introduction

[2] In subduction zones, great earthquakes (moment magnitude, $M_w > 8.0$) are generated along a plate boundary megathrust and are often accompanied by destructive tsunamis such as the 2004 Sumatra earthquake [*Lay et al.*, 2005]. In accretionary margins, a large out-of-sequence fault system (the "megasplay" fault) commonly branches from the megathrust and intersects the seafloor along the lower slope of the margin [*Moore et al.*, 2007, and references therein]. Theoretical studies argue that an earthquake rupture tends to branch along such a megasplay fault system [*Kame et al.*, 2003]. In the Nankai accretionary margin offshore the Kii Peninsula, southwest Japan, the extent of the 1944 Tonankai earthquake ($M_w = 8.1$) coseismic rupture estimated from tsunami and seismic waveform inversions suggests that the earthquake rupture propagated along a megasplay fault [*Tanioka and Satake*, 2001; *Kikuchi et al.*, 2003] (Figures 1a and 1b).

[3] Recently, the Integrated Ocean Drilling Program (IODP) Expedition 316 drilled into the shallow portion of the megasplay fault zone at Site C0004 (Figures 1a and 1b). The megasplay fault zone is developed at 258–308 mbsf (meters below sea floor) and is composed of brecciated and fractured mudstone and volcanic ash deposits [*Expedition 316 Scientists*, 2009]. This fault zone exhibits the slip localization along ~10-mm-thick dark gouges in the microbreccia [*Ujiie et al.*, 2008] (Figure 1c). The high vitrinite reflectance in the dark gouge relative to the ambient microbreccia suggests the generation of frictional heat at a temperature of several hundred degrees centigrade along the localized slip zone, even at shallow depths [*Sakaguchi et al.*, 2009]. Here, we report the results of high-velocity friction experiments on the megasplay fault material taken from immediately below (~5 cm) the dark gouge at 271 mbsf and resulting microstructures. The megasplay fault material is derived from hemipelagic muds with minor interbedded volcanic ash and is composed of quartz, plagioclase, smectite, illite, chlorite, and minor calcite with its total clay mineral content ranging from 52.9% to 65.4% [*Expedition 316 Scientists*, 2009]. Knowledge of high-velocity frictional properties of the megasplay fault material is crucial for understanding whether the megasplay fault efficiently transfers displacement toward the seafloor and fosters tsunamigenesis during a subduction earthquake. The high-velocity frictional properties obtained from our study may be widely applicable to earthquake rupture propagation through mature faults because these faults commonly contain a considerable amount of clay minerals in their core [*Faulkner et al.*, 2010].

2. Methods

[4] High-velocity friction experiments were conducted on the clay-rich fault gouge at an equivalent slip rate (V_e) of 1.27 m/s and normal stresses (σ_n) of 0.6–2.0 MPa under dry (equilibrate with room humidity) and wet (water saturated) conditions by using the new rotary-shear high-velocity friction apparatus in Kyoto University [*Hayashi and Tsutsumi*, 2010]. The basic design of this apparatus is similar to that described by *Shimamoto and Tsutsumi* [1994]. However, the orientations of their revolution axes are different: the revolution axis of the new apparatus is vertical, whereas that of the old apparatus is horizontal. The samples were disaggregated using a pestle, oven-dried at 60 °C for 24 h, and sieved to obtain an experimental fault gouge with a diameter of less than 0.17 mm. For each experiment, 0.5 g of the gouge was placed between a pair of solid cylindrical granite specimens with a diameter of 25 mm. The end surfaces of the granite specimens were ground with #80 SiC powders to prevent slip along the boundaries between the gouge and the granite specimens. Upon application of σ_n for 0.5 h (before shearing), the gouge thickness was ~0.8 mm. The weight of the fault gouge is half of that used for the previous high-velocity friction experiments on fault gouges [*Mizoguchi et al.*, 2009,

[1]Doctoral Program in Earth Evolution Sciences, Graduate School of Life and Environmental Sciences, University of Tsukuba, Tsukuba, Japan.
[2]Division of Earth and Planetary Sciences, Graduate School of Science, Kyoto University, Kyoto, Japan.

0094-8276/10/2010GL046002

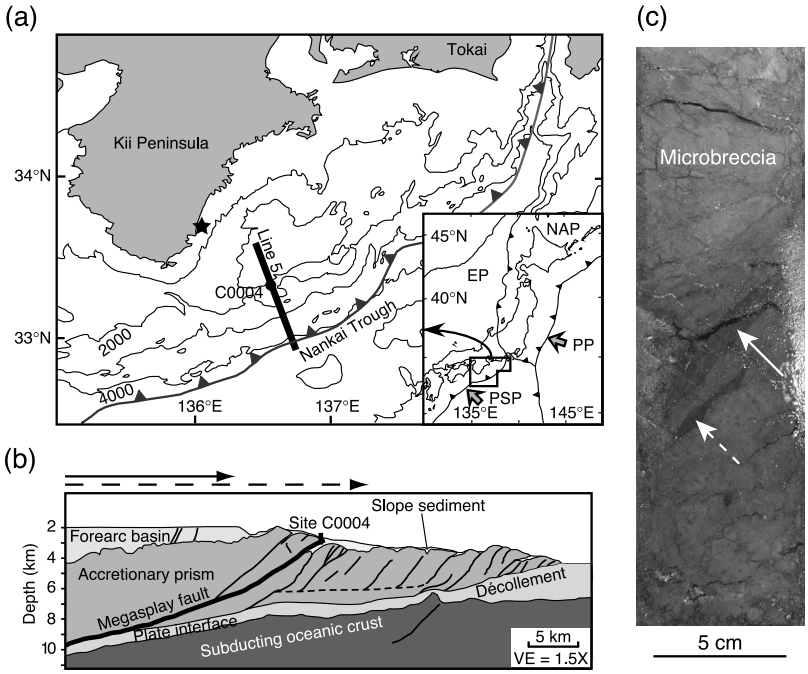

Figure 1. Megasplay fault in Nankai subduction zone. (a) Map of Nankai accretionary margin offshore Kii Peninsula showing location of drill site C0004 and epicenters of 1944 Tonankai earthquake (star). Inset: PSP = Philippine Sea plate, EP = Eurasian plate, PP = Pacific plate, and NAP = North American plate. (b) Profile of megasplay fault along Line 5 in Figure 1a. Solid and broken arrows indicate the extent of 1944 Tonankai earthquake coseismic rupture from tsunami and seismic waveform inversions, respectively. (c) Photograph of split core showing dark gouge (white arrow) and fragment of dark gouge (broken white arrow) in microbreccia.

and references therein] in order to achieve relatively high temperatures in the fault gouge because of the relatively high heat production rate. In the wet tests, 0.2 ml of distilled water was added to the gouge. A hollow-cylindrical Teflon sleeve surrounded the fault to prevent gouge extrusion during rotation. The assembly was set in the apparatus in which the upper cylinder remains stationary while the lower one is rotated by a servomotor. The rotation of the motor was transmitted to the specimen through an electromagnetic clutch. During the experiments, the humidity was monitored by a moisture sensor, and the temperature was measured by a thermocouple installed on the stationary side at a distance of 9.5 mm from the boundary between the fault gouge and the granite specimen. We also conducted numerical modeling to determine the temperature evolution and distribution in a section of the granite-gouge-Teflon sleeve using the finite element method proposed by *Kuroda* [2001] (see auxiliary material and *Mizoguchi et al.*, 2009 for details).[1]

3. Results

3.1. Frictional Properties and Temperatures During High-Velocity Shearing

[5] Typical experimental results for the dry and wet tests are shown in Figures 2a and 2b, respectively (e.g., see also auxiliary material showing the reproducibility of the experimental results). In the dry tests, the peak friction is in the range of 0.6–0.7. This is followed by a decrease in the friction over the slip weakening distances (D_c) of 2.66–13.84 m toward a steady-state friction of 0.2–0.3. D_c decreases with an increase in σ_n (Figure 2a and auxiliary material). The fault gouge was compacted immediately after the onset of shearing and then dilated. The end of slip weakening corresponds to the end of gouge dilation (Figure 2a and auxiliary material). Humidity increases with displacement.

[6] In the wet tests, the peak friction is reduced to 0.3–0.5. The steady-state friction of 0.1–0.2 is established almost immediately, demonstrating that irrespective of σ_n, D_c is very small (less than 0.2–0.3 m) (Figure 2b and auxiliary material). Compared to the dry tests, the wet tests show relatively small dynamic stress drops, slip weakening distance, fracture energy, and initial compaction (Figure 2 and auxiliary material). After initial compaction, the compaction rate is low until the end (clutch off) of the wet tests. The wet tests conducted at σ_n of 0.6 and 1.0 MPa show transient gouge dilation during the steady-state friction; this feature is not observed for the tests conducted at σ_n of 1.5 and 2.0 MPa (Figure 2b and auxiliary material). The humidity first decreases and then increases (auxiliary material). The increase in the humidity under wet conditions occurred before or after the end of shearing, which appears to depend on the elapsed time.

[7] Under dry and wet conditions, the temperatures in the fault gouge increase rapidly during slip weakening, but their increase rates decrease gradually during the steady-state friction (Figures 2a and 2b). The temperatures in the fault gouge at distances of 3.75 mm and 11 mm from the revolution axis at the end of the experiments under the dry conditions are 249–343°C and 375–572°C, respectively, whereas those

[1] Auxiliary materials are available in the HTML. doi:10.1029/2010GL046002.

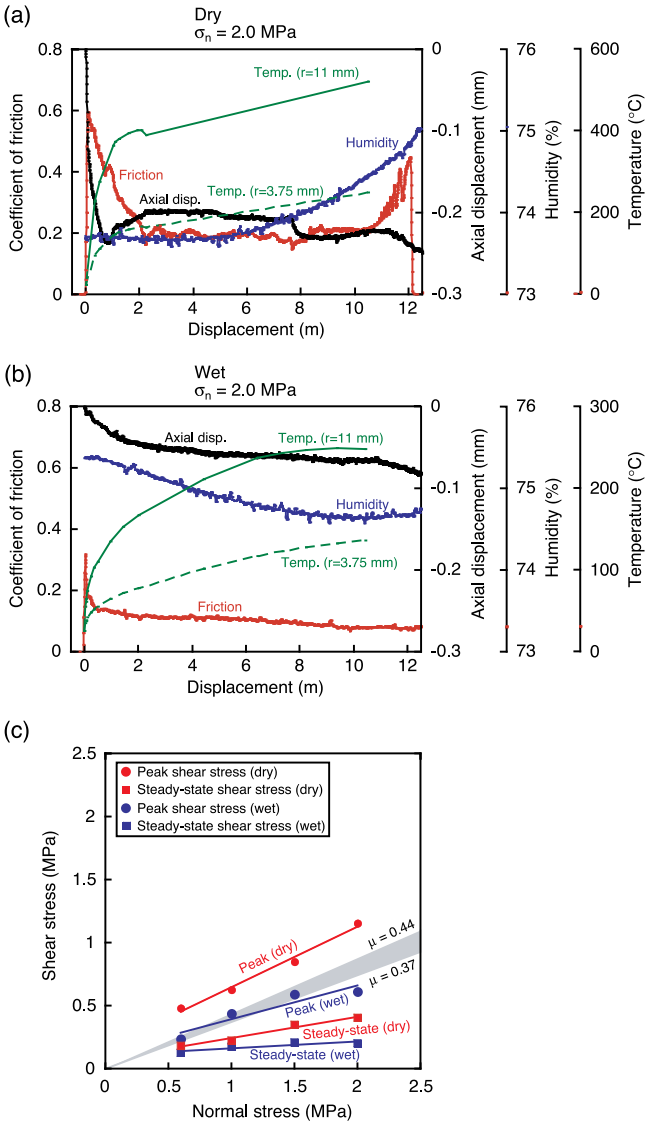

Figure 2. Experimental results. Coefficient of friction, axial displacement, humidity, and numerically calculated temperatures in the fault gouge at 3.75 mm and 11 mm from the revolution axis versus the displacement at σ_n of 2.0 MPa under (a) dry and (b) wet conditions. Temperature in fault gouge is calculated until the end (i.e., disengagement of the clutch) of experiments. (c) Peak shear stress and steady-state shear stress versus normal stress under dry and wet conditions. Steady-state stress is the average of the shear stresses during last 5 s before clutch off. Frictional strength of the megasplay fault material at low slip rates [*Ikari et al.*, 2009] is plotted in gray.

under the wet conditions are 136–210°C and 248–326°C, respectively. We note here that the calculated temperatures for the dry tests do not account for the slip localization during the sliding (described later); thus, the calculated temperatures for the dry tests would be underestimated.

[8] The dependence of the shear stress at the peak (τ_p) and steady-state (τ_{ss}) on σ_n can be expressed by the following linear relationships: $\tau_p = 0.16 + 0.48\ \sigma_n$ and $\tau_{ss} = 0.07 + 0.17\ \sigma_n$ for the dry tests, and $\tau_p = 0.13 + 0.27\ \sigma_n$ and $\tau_{ss} = 0.11 + 0.06\ \sigma_n$ for the wet tests. τ_p in the dry and wet tests are higher than and equivalent to the frictional strength of the Nankai megasplay fault materials at low slip rates (<100 μm/s) under a saturated condition, respectively [*Ikari et al.*, 2009]; however, τ_{ss} is well below the frictional strength at low slip rates in the case of both dry and wet conditions, with τ_{ss} in our wet tests being nearly independent of σ_n (Figure 2c).

3.2. Microstructures After High-Velocity Shearing

[9] The microstructures of the fault gouge were examined with an optical microscope and a scanning electron microscope. The microstructures after the dry tests are marked by the localized slip zone with a thickness of less than 0.2 mm along the boundary between the gouge and the granite specimen and the presence of spherical aggregates in the optically isotropic matrix (Figures 3a and 3b). The localized slip zone shows the alignment of extremely fine-grained clay particles along the zone. The spherical aggregates are defined by clasts of quartz and plagioclase surrounded by a cortex of concentric clay layer, corresponding to the clay-clast aggregates (CCA) [*Boutareaud et al.*, 2008]. An X-ray diffraction (XRD) analysis of the powdered gouge samples was performed before and after the experiments, and the analysis results revealed that the X-ray diffraction peaks observed for illite, chlorite, and calcite before the experiments disappeared after the experiments (auxiliary material).

[10] The foliated zone defined by the preferred orientation of the clay particles is developed in the gouge layer after the wet tests (Figure 3c). Compared to the localized slip zone developed under dry conditions, the foliated zone is thick (thickness: 0.25–0.45 mm), and there is no pronounced size reduction of clay minerals, consistent with a small fracture energy (Figure 2b). In the peripheral part of the cylinder where the rotation velocity ($V = 2\pi rR/60$, where r and R are the radius of the specimen and the revolution rate of the motor, respectively) ranges from 0.62 to 1.66 m/s, the large grains are concentrated in the upper part of the gouge layer (Figure 3d). This grain size segregation occurs symmetrically about the rotational axis and tends to develop in the foliated zone (Figure 3c).

4. Discussion and Conclusions

[11] In the dry tests (e.g., Figure 2a and auxiliary material), slip weakening is closely correlated to gouge dilation. Further, the calculated temperatures in the peripheral part of the gouge layer during slip weakening (well above 200°C in all dry tests) suggest that clay minerals can release their absorbed and interlayer water [*Brindley and Brown*, 1980; *Deer et al.*, 1992]. Using the water phase diagram [*Fisher*, 1976], the temperatures for water phase transition from liquid to vapor at 0.6–2.0 MPa are estimated as 159–213°C. Thus, the water dehydrated from the clay minerals vaporized, resulting in an increase in the water volume by a factor of 10. The development of CCA in the gouge is also consistent with water vaporization [*Boutareaud et al.*, 2008], and the increase in humidity during the dry tests reflects the leak of vaporized water from the gouge layer. The production rate of water vaporization is likely to be higher than the radial leaking rate of vapor, resulting in the dilation of the gouge layer. Therefore, the slip weakening during the dry tests is caused by the fault gouge expansion associated with the liquid-vapor transition of water (i.e., thermal pressurization [*Sibson*, 1973]),

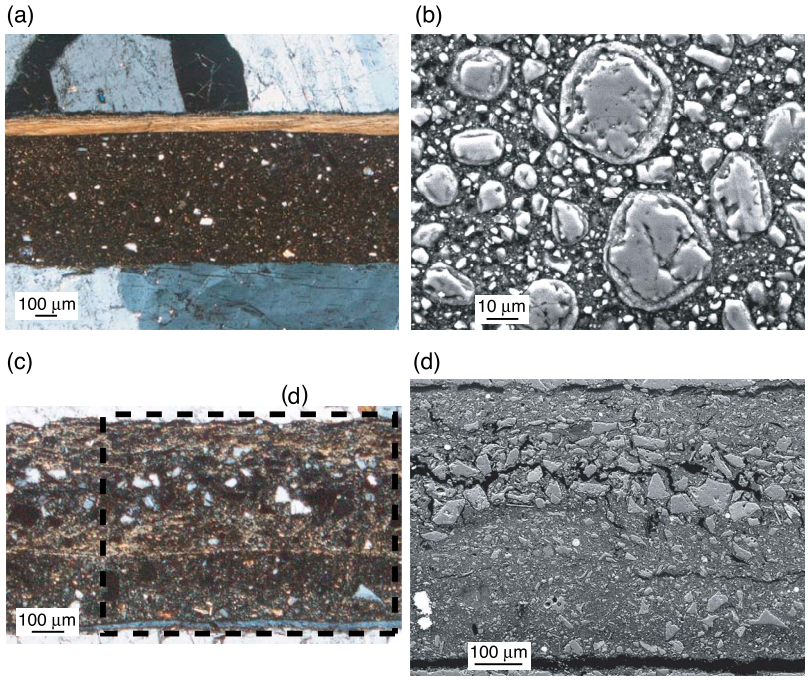

Figure 3. Typical microstructures formed after dry (a and b) and wet (c and d) tests. (a) Fault gouge composed of localized slip zone and random distribution of clasts in optically isotropic, dark matrix. Cross-polarized light. (b) Back-scattered electron (BSE) images of clay-clast aggregates. (c) Grain size segregation in foliated zone. Cross-polarized light. (d) BSE image of grain size segregation in the upper part of the gouge layer. Location of the image is shown in Figure 3c.

which is derived from the dehydration of clay minerals by frictional heating.

[12] The initial compaction of the fault gouge during the rapid slip weakening in the wet tests is markedly smaller than that during the corresponding slip in the dry tests (Figures 2a and 2b and auxiliary material). This would be induced by the pore-fluid pressurization due to the shear-enhanced compaction of the water-saturated fault gouge sandwiched between a pair of impermeable granite specimens. On the other hand, the rapid increase in temperature of the gouge during the rapid slip weakening implies that fluid pressurization is related to the generation of frictional heat. The calculated temperature in the peripheral part of the gouge layer (well below 159–213°C) and the absence of gouge dilation during slip weakening suggest that the dehydration of the clay minerals and water vaporization are not responsible for the rapid weakening of the wet gouge. Therefore, the rapid slip weakening during the wet tests most probably represents the pore-fluid pressurization due to a combination of shear-enhanced compaction and frictional heating.

[13] A very weak dependence of τ_{ss} on σ_n under wet conditions suggests that the gouge behaved like a fluid. In such a case, the resultant foliated zone in the gouge layer may represent the flow textures, and the spatial distribution of the grain size segregation in the gouge layer suggests the flow sorting. According to Bagnold's law [*Bagnold*, 1954], the dispersive pressure (P) associated with granular collision in a granular-fluid shear flow is proportional to the square of the shear rate ($d\gamma/dt$):

$$P \propto \rho(\lambda D)^2 \left(\frac{d\gamma}{dt}\right)^2 \approx \rho(\lambda D)^2 \left(\frac{V}{w}\right)^2 \approx \rho(\lambda D V)^2 \qquad (1)$$

where ρ is the density of the granular-fluid materials, λ is the linear grain concentration defined as the ratio of the grain diameter to the mean free separation distance between the grains, D is the grain diameter, and w is the thickness of the fault gouge (nearly constant throughout the cylinder). Equation (1) indicates that the difference in P between the large and the small grains is increased toward the margin of the specimen, where V is the highest. In the fault gouge under a granular-fluid shear flow at high slip rates, the voids tend to be formed around large grains because of the difference in P. On the basis of the size difference, it is obvious that the small grains have a higher probability of filling these voids than the larger ones [*Rosato et al.*, 1987]. The large grains are moved upward as the smaller grains fill the voids by the downward movement under gravity. Such grain size segregation is comparable to the Brazil-nut effect [*Williams*, 1976] (i.e., when grain mixtures are shaken or collided, the larger grains rise on top of the smaller ones). The spatial distribution of the grain size segregation in the fault gouge is due to the Brazil-nut effect caused by the large difference in P between the large and the small grains at high shear rates. The grain size segregation formed by the Brazil-nut effect associated with granular collision in a granular-fluid shear flow will be a new microstructural evidence for the occurrence of high slip rates.

[14] Recently, *Ferri et al.* [2010] conducted high-velocity (V_e = 1.31 m/s) friction experiments on smectite-rich gouges under dry and wet conditions using the apparatus described by *Shimamoto and Tsutsumi* [1994]. Our experimental results (gouge dilation) and microstructures (CCA) obtained under dry conditions are similar to their dry tests results; however, *Ferri et al.* [2010] did not report grain size segregation in the gouge layer after their wet tests. This may reflect the

difference in the orientations of the revolution axes between the apparatuses. Because the Brazil-nut effect requires a downward movement of small grains by gravity, grain size segregation brought by the Brazil-nut effect is likely to occur in an apparatus with a vertical revolution axis. The important implication for natural faults is that the flow sorting induced by the Brazil-nut effect is more likely to occur in low- to moderate-dipping faults than in vertical strike-slip faults. In fact, grain size segregation has recently been reported in a 2-cm-thick clay-rich fault gouge in the Chelungpu thrust fault, which is interpreted as a record of the thermal pressurization-induced fluidization caused during the 1999 Taiwan Chi-Chi earthquake [*Boullier et al.*, 2009].

[15] A clay-rich fault gouge commonly exhibits velocity-strengthening behavior at low slip rates (<100 μm/s); thus, the nucleation of a seismic slip is unlikely in shallow portions of faults [e.g., *Morrow et al.*, 1992; *Ikari et al.*, 2009]. τ_p during high-velocity friction experiments on a clay-rich fault zone material under dry and wet conditions is relatively high and equivalent to the frictional strength of the same fault zone material at low slip rates, respectively (Figure 2c). Once the stabilizing slip property and frictional peak are overcome, our results imply that an earthquake rupture from deeper portions propagates easily through the clay-rich fault gouge in the shallow fault zone by high-velocity weakening associated with fluid pressurization and frictional heat. The growth of the earthquake rupture may be controlled by high-velocity weakening; if this works in shallow portions of the megasplay faults, it would enhance tsunami generation.

[16] **Acknowledgments.** This research used samples and data provided by IODP. We are grateful to members of the Expedition 316 Scientists, and the captain, drilling crew, and technicians of the D/V Chikyu for their support and cooperation onboard the ship. We gratefully acknowledge Takahiro Hatano and Yuri Fialko for their helpful discussions. We thank GRL editor Ruth Harris, Matt Ikari, and anonymous reviewer for their thoughtful comments. This research was funded by Grant-in-Aid for Scientific Research (B) from JSPS (21340150) and by Grant-in-Aid for Scientific Research on Innovative Areas from MEXT (21107005).

References

Bagnold, R. A. (1954), Experiments on a gravity-free dispersion of large solid spheres in a Newtonian fluid under shear, *Proc. R. Soc. London, Ser. A*, *225*, 49–63, doi:10.1098/rspa.1954.0186.

Boullier, A.-M., E.-C. Yeh, S. Boutareaud, S.-R. Song, and C.-H. Tsai (2009), Microscale anatomy of the 1999 Chi-Chi earthquake fault zone, *Geochem. Geophys. Geosyst.*, *10*, Q03016, doi:10.1029/2008GC002252.

Boutareaud, S., D.-G. Calugaru, R. Han, O. Fabbri, K. Mizoguchi, A. Tsutsumi, and T. Shimamoto (2008), Clay-clast aggregates: A new textural evidence for seismic fault sliding?, *Geophys. Res. Lett.*, *35*, L05302, doi:10.1029/2007GL032554.

G. W. Brindley, and G. Brown (Eds.) (1980), *Crystal Structure of Clay Minerals and their X-Ray Identification*, *Mineral. Soc. Monogr.*, 5, 495 pp.

Deer, W. A., R. A. Howie, and J. Zussman (1992), *An Introduction to the Rock-Forming Minerals*, 2nd ed., 696 pp., Longmans, London, U. K.

Expedition 316 Scientists (2009), Expedition 316 Site C0004, in *NanTroSEIZE Stage 1: Investigations of Seismogenesis, Nankai Trough, Japan*, *Proc. Integr. Ocean Drill. Program*, 314/315/316, doi:10.2204/iodp.proc.314315316.133.2009.

Faulkner, D. R., C. A. L. Jackson, R. J. Lunn, R. W. Schlische, C. A. J. Wibberley, and M. O. Withjack (2010), A review of recent developments concerning the structure, mechanics and fluid flow properties of fault zones, *J. Struct. Geol.*, *32*, 1557–1575, doi:10.1016/j.jsg.2010.06.009.

Ferri, F., G. Di Toro, T. Hirose, and T. Shimamoto (2010), Evidence of thermal pressurization in high velocity friction experiments on smectite-rich gouges, *Terra Nova*, *22*, 347–353, doi:10.1111/j.1365-3121.2010.00955.x.

Fisher, J. R. (1976), The volumetric properties of H_2O—A graphical portrayal, *J. Res. U.S. Geol. Surv.*, *4*, 189–193.

Hayashi, T., and A. Tsutsumi (2010), Deformation textures and mechanical behavior of a hydrated amorphous silica formed along an experimentally produced fault in chert, *Geophys. Res. Lett.*, *37*, L12305, doi:10.1029/2010GL042943.

Ikari, M. J., D. M. Saffer, and C. Marone (2009), Frictional and hydrologic properties of a major splay fault system, Nankai subduction zone, *Geophys. Res. Lett.*, *36*, L20313, doi:10.1029/2009GL040009.

Kame, N., J. R. Rice, and R. Dmowska (2003), Effects of prestress state and rupture velocity on dynamic fault branching, *J. Geophys. Res.*, *108*(B5), 2265, doi:10.1029/2002JB002189.

Kikuchi, M., M. Nakamura, and K. Yoshikawa (2003), Source rupture process of the 1944 Tonankai earthquake and the 1945 Mikawa earthquake derived from low-gain seismograms, *Earth Planets Space*, *55*, 159–172.

Kuroda, H. (2001), *Two-Dimensional Heat Flow Analysis Program Using Finite Element Method* (in Japanese), 255 pp., CQ, Tokyo.

Lay, T., et al. (2005), The great Sumatra-Andaman earthquakes of 26 December 2004, *Science*, *308*, 1127–1133, doi:10.1126/science.1112250.

Mizoguchi, K., T. Hirose, T. Shimamoto, and E. Fukuyama (2009), High-velocity frictional behavior and microstructure evolution of fault gouge obtained from Nojima fault, southwest Japan, *Tectonophysics*, *471*, 285–296, doi:10.1016/j.tecto.2009.02.033.

Moore, G. F., N. Bangs, A. Taira, S. Kuramoto, E. Pangborn, and H. J. Tobin (2007), Three-dimensional splay fault geometry and implications for tsunami generation, *Science*, *318*, 1128–1131, doi:10.1126/science.1147195.

Morrow, C., B. Radney, and J. Byerlee (1992), Frictional strength and effective pressure law of montmorillonite and illite clays, in *Fault Mechanics and Transport Properties of Rocks*, *Int. Geophys. Ser.*, vol. 51, edited by B. Evans and T.-F. Wong, pp. 69–88, Academic, London.

Rosato, A., K. J. Strandburg, F. Prinz, and R. H. Swendsen (1987), Why the Brazil nuts are on top: Size segregation of particulate matter by shaking, *Phys. Rev. Lett.*, *58*, 1038–1040, doi:10.1103/PhysRevLett.58.1038.

Sakaguchi, A., F. M. Chester, O. Fabbri, D. L. Goldsby, C. Li, G. Kimura, A. Tsutsumi, K. Ujiie, A. Yamaguchi, and D. Curewitz (2009), Paleothermal condition of the shallow mega-splay fault based on vitrinite reflectance: Core analysis of IODP NanTroSEIZE stage 1, *Eos Trans. AGU*, *90*(52), Fall Meet. Suppl., Abstract T12A-08.

Shimamoto, T., and A. Tsutsumi (1994), A new rotary-shear high-velocity frictional testing machine: Its basin design and scope of research (in Japanese with English abstract), *Struct. Geol.*, *39*, 65–78.

Sibson, R. H. (1973), Interactions between temperature and pore-fluid pressure during earthquake faulting and a mechanism for partial or total stress relief, *Nature*, *243*, 66–68.

Tanioka, Y., and K. Satake (2001), Detailed coseismic slip distribution of the 1944 Tonankai earthquake estimated from tsunami waveforms, *Geophys. Res. Lett.*, *28*, 1075–1078, doi:10.1029/2000GL012284.

Ujiie, K., F. M. Chester, O. Fabbri, C. Li, A. Yamaguchi, X. Su, G. Kimura, E. J. Screaton, and D. Curewitz (2008), Characteristics of the fault rocks at the shallow portion of the megasplay fault system and the frontal thrust in the Nankai accretionary prism off Kumano, *Eos Trans. AGU*, *89*(53), Fall Meet. Suppl., Abstract T21F-02.

Williams, J. C. (1976), The segregation of particulate materials. A review, *Powder Technol.*, *15*, 245–251, doi:10.1016/0032-5910(76)80053-8.

A. Tsutsumi, Division of Earth and Planetary Sciences, Graduate School of Science, Kyoto University, Kita-shirakawa, Sakyo-ku, Kyoto 606-8502, Japan.

K. Ujiie, Doctoral Program in Earth Evolution Sciences, Graduate School of Life and Environmental Sciences, University of Tsukuba, 1-1-1 Tennodai, Tsukuba 305-0006, Japan. (kujiie@geol.tsukuba.ac.jp)